Experimental validation of a sampled-data passivity-based controller for coordination of converters in a fuel cell system

Mickael Hilairet, Olivier Bethoux, Malek Ghanes, Valentin Tanasa, Jean-Pierre Barbot, Dorothée Normand-Cyrot

Experimental Validation of a Sampled-Data Passivity-Based Controller for Coordination of Converters in a Fuel Cell System

Mickaël Hilairet, *Member, IEEE*, Olivier Béthoux, *Member, IEEE*, Malek Ghanes, *Member, IEEE*, Valentin Tanasa, *Member, IEEE*, Jean-Pierre Barbot, *Senior Member, IEEE*, and Marie-Dorothée Normand-Cyrot, *Fellow, IEEE*

***Abstract*—This paper deals with the control of a hybrid source combining a proton exchange membrane fuel cell and supercapacitors. To achieve this objective, an interconnection and damping assignment passivity-based control in a sampled-data context is implemented. This paper first details with this new controller and shows that it ensures the stabilization of the hybrid system at its desired equilibrium point under large range of sampling periods. These considerations are followed by a detailed discussion on experimental results achieved on a 1.2-kW test bench.**

***Index Terms*—Experimentation, fuel cell (FC), interconnection and damping assignment passivity-based control (IDA-PBC) methodology, port-controlled Hamiltonian systems, power management, sampled-data controller, supercapacitors.**

I. Introduction

CONSIDERATION of atmospheric pollution becomes a significant public health problem in industrializing countries as their automotive market develops. Hence, in these countries and in advanced industrial countries, electric vehicles are beginning to play a key role to comply with environmental standards, which are becoming more stringent. To develop environmentally friendly vehicles compatible with the current requirements concerning automotive sector, the combination of hydrogen tank and fuel cell (FC) is a promising path. It ensures no local emission, the traction power, and a high cruising range. To improve this solution energy efficiency, a bidirectional storage device has to be added: it enables to recover braking energy and assist the FC during rapid demand power changes, which significantly increases the FC lifetime [1]–[16]. For this function, supercapacitors (SCs) are good candidates since they have a high power density and are able to produce a large number of charge/discharge cycles.

Many power structures can combine FC and SC power sources, as mentioned in [17]. The one based on the double-converter structure [18] enables both energy management and bus voltage regulation, which is particularly important for some applications such as electric vehicles. This paper is based on this structure. The power demand can be supplied by both sources. The SCs can harvest the load regenerative power and the FC transient excess power delivery. Indeed, for life span reasons, FC has to avoid idle functioning or sharp power changes.

Power management of this system relies on frequency decoupling. The controller has to meet three main objectives: first, respect the FC dynamic by limiting FC power slope regardless of load demand; second, comply with the load demand; and third, control the SC charge. Among the many techniques that are available for this application (see, for instance, [19], for a short bibliography), passivity-based controllers are attractive because they guarantee stability properties [20]. The practical implementation is actually based on a microcontroller, and hence depends on signals sampling and zero-order hold (ZOH) devices. It consequently involves discrete theory. In order to best approximate a pure continuous controller (which is called emulation process in a sampled-data context), the implementation may use either very small sampling period or a set of low-value gains [19], [21]. Both cases do not offer optimal solutions. The first case requires a microcontroller with high performances (fast analog-to-digital conversion and a high clock frequency of the control unit), whereas the second leads to poor hybrid system performance with respect to selected criteria. The aim of this paper is to prove that a pure digital passivity-based controller can fulfill the hybrid source requirement, although the imposed sampling frequency of the control process is quite low.

M. Hilairet was with the Laboratoire de Génie Electrique de Paris, University of Paris-Sud, 91192 Paris, France. He is now with the "Franche-Comté Electronique Mécanique Thermique et Optique-Sciences et Technologies," University of Franche-Comté, 90000 Belfort, France (e-mail: mickael.hilairet@univ-fcomte.fr).

O. Béthoux is with the Laboratoire de Génie Electrique de Paris, Université Paris-Sud, 91192 Paris, France (e-mail: olivier.bethoux@lgep.supelec.fr).

M. Ghanes is with the Electronic and Control Systems Laboratory, École Nationale Supérieure de l'Électronique et de ses Applications, 95014 Paris, France (e-mail: Malek.Ghanes@ensea.fr).

V. Tanasa is with the University Politehnica of Bucharest, 060042 Bucharest, Romania, and also with the Railway Transportation Division, Thales Systems Romania, 060044 Bucharest, Romania (e-mail: valentin.tanasa@cti.pub.ro).

J.-P. Barbot is with the Electronic and Control Systems Laboratory, École Nationale Supérieure de l'Électronique et de ses Applications, 95014 Paris, France, and also with the Project Team Non-A, Institut National de Recherche en Informatique et en Automatique, 59650 Lille, France (e-mail: barbot@ensea.fr).

M.-D. Normand-Cyrot is with the Laboratoire des Signaux et Systèmes, Centre National de la Recherche Scientifique, 91192 Paris, France (e-mail: Dorothee.Normand-Cyrot@lss.supelec.fr).

Motivated by a recent theoretical result in [22], this study builds on a previous theoretical study, which demonstrates that a direct sampled-data controller based on the interconnection and damping assignment passivity [interconnection and damping assignment passivity-based control (IDA-PBC)] theory can successfully achieve stabilization without any overcurrent [23] under large sampling time.

The main motivation of this work is the design of a controller that:

1) ensures the stability of the whole system;
2) generalizes regular linear controller such as PI controller (see, for instance, [19, eqs. (12) and (13)], which could be useful);
3) integrates the knowledge of the system to reproduce regular controllers;
4) allows large sampling time without degrading the performances.

Items 1–3 are detailed in [19] for the same power architecture based on the double-converter structure, whereas item 4 is addressed in this paper. As a result, the four items have been followed and carried out leading to a complete procedure for designing a controller enabling the real-time coordination of many converters. The latter has been implemented on a test bench with two sources and a load and compared with the analog passive approach of [19].

This paper is organized as follows. In Section II, the modeling of hybrid source and the background of continuous IDA-PBC theory are recalled (see [19] for more details). Section III details the proposed sampled-data passivity-based controller. Section IV shows and discusses the actual experimental results achieved on a reduced-scale test bench based on a 1.2-kW Nexa Ballard FC and compared it with the analog passive approach of [19]. Section V provides concluding remarks.

II. System Architecture

A. Problem Settlement

The hybrid source consists of a low-transient unidirectional power flow source (FC) and a fast-transient bidirectional power flow source (SC) interconnected by a two-converter structure proposed in [18], [19], and [23] and represented in Fig. 1. Such architecture permits the control scheme to properly manage the different powers. The control of the SCs converter has to regulate the dc bus voltage at a constant value equal to its reference v_b^*, whereas the control of the FC converter has to drive the SCs state of charge toward its constant target value. To work properly, the control scheme is divided in three subblocks.

- A digital nonlinear controller (outer loop) controls the dc bus voltage and the charge of SCs by computing current references $i_{\rm fc}^*$ and $i_{\rm sc}^*$ values. Saturations ensure that their values do not exceed $[0; i_{\rm fc\ max}]$ and $[-i_{\rm sc\ max}; +i_{\rm sc\ max}]$, which are defined in order to protect FC, SCs, and converters.
- Two fast inner proportional–integral (PI) current loops featuring antiwindup compensation schemes ensure that whatever load requirements, $i_{\rm fc}$ and $i_{\rm sc}$ go rapidly to their reference values $i_{\rm fc}^*$ and $i_{\rm sc}^*$, respectively, which are imposed by the outer loop, which is the digital IDA-PBC controller in this study. The outputs of both PI controllers define the duty cycles $\alpha_{\rm fc}$ and $\alpha_{\rm sc}$ of the two converters.

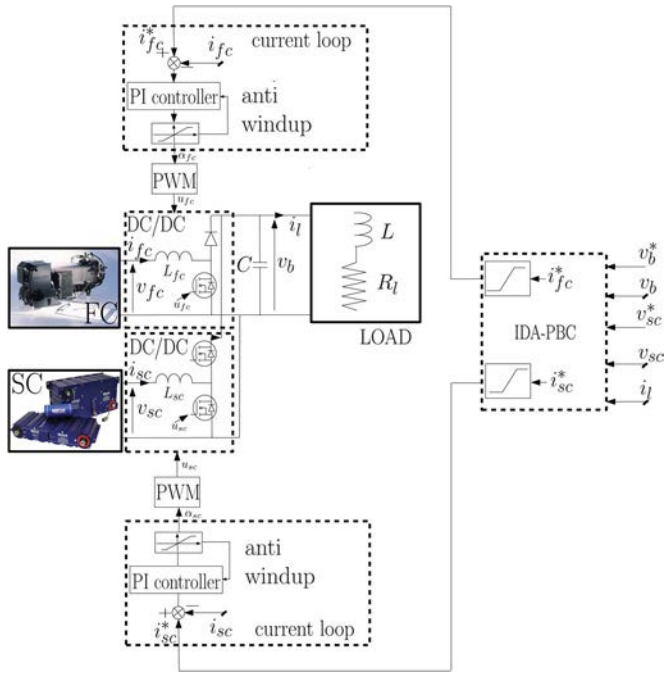

Fig. 1. Studied system with its associated control scheme.

The complete "fuel cell—supercapacitors" system with the associated control scheme is represented in Fig. 1. The whole system is described by a fifth-order nonlinear state-space model called *singular perturbed system* [24], because of the timescale difference between the voltages and the currents. Consequently, assuming that currents $i_{\rm fc}$ and $i_{\rm sc}$ are instantaneous compared with voltages v_b and $v_{\rm sc}$, the fifth-order differential system degenerates to a third-order differential system as follows [19]:

$$\begin{aligned}\frac{d}{dt}v_b(t) &= \frac{1}{C}\left(\frac{v_{\rm fc}(t)}{v_b(t)}i_{\rm fc}^*(t) + \frac{v_{\rm sc}(t)}{v_b(t)}i_{\rm sc}^*(t) - i_l(t)\right)\\ \frac{d}{dt}v_{\rm sc}(t) &= -\frac{i_{\rm sc}^*(t)}{C_{\rm sc}}\\ \frac{d}{dt}i_l(t) &= \frac{-R_l(t)i_l(t) + v_b(t)}{L}\end{aligned} \tag{1}$$

with $x_r(t) = [x_1(t); x_2(t); x_3(t)]^T = [v_b(t); v_{\rm sc}(t); i_l(t)]^T$, control reference inputs $u_r(t) = [i_{\rm fc}^*(t); i_{\rm sc}^*(t)]^T$, and measures $y_r(t)$ and $z_r(t)$, where $y_r(t) = [v_b(t); v_{\rm sc}(t); i_l(t)]^T$, and $z_r(t) = [i_{\rm fc}(t); i_{\rm sc}(t); v_{\rm fc}(t)]^T$.

Remark 1: The charge has been considered as a $R_l L$ load in order to represent the current as a time-varying profile without abrupt change by a proper value of the inductance L.

B. IDA-PBC Outer-Loop Controller Design

The IDA-PBC needs to handle the state $x_r(t)$ to the reference equilibrium point $x_r^*(t) = [v_b^*(t); v_{\rm sc}^*(t); (v_b^*(t)/R_l(t))]$, with $v_b^*(t)$ and $v_{\rm sc}^*(t)$ being the dc bus and SCs reference voltages, respectively.

A storage energy function H_d is defined as $H_d(\tilde{x}_r(t)) = (1/2)\tilde{x}_r(t)^T Q \tilde{x}_r(t)$ with $\tilde{x}_r(t) = x_r(t) - x_r^*(t)$ and $Q = \mathrm{diag}(C, C_{\mathrm{sc}}, L)$, so that this function is equal to zero at the equilibrium point $x_r^*(t)$. In this context, the dynamical error equation is as follows:

$$\dot{\tilde{x}}_r(t) = [\mathcal{J} - \mathcal{R}]\nabla H_d(\tilde{x}_r(t)) + g(x_r(t))\, u_r(t) + d(t) \quad (2)$$

$$y_r(t) = g^T(x_r(t))\, \nabla H_d(\tilde{x}_r(t)) \quad (3)$$

with

$$\mathcal{J} - \mathcal{R} = \begin{bmatrix} 0 & 0 & -\frac{1}{LC} \\ 0 & 0 & 0 \\ \frac{1}{LC} & 0 & -\frac{R_l}{L^2} \end{bmatrix}$$

$$\nabla H_d(\tilde{x}_r(t)) = [\, C\tilde{v}_b(t) \quad C_{\mathrm{sc}}\tilde{v}_{\mathrm{sc}}(t) \quad L\tilde{i}_l(t)\,]^t$$

$$g(x_r(t)) = \begin{bmatrix} \frac{v_{\mathrm{fc}}(t)}{Cv_b(t)} & \frac{v_{\mathrm{sc}}(t)}{Cv_b(t)} \\ 0 & -\frac{1}{C_{\mathrm{sc}}} \\ 0 & 0 \end{bmatrix}$$

$$d(t) = \begin{bmatrix} -\frac{i_l^*(t)}{C} \\ 0 \\ 0 \end{bmatrix}.$$

An algebraic equation needs to be solved in order to obtain the controller, with the constraint of skew symmetry and positive semidefiniteness of $\mathcal{J}_d$ and $\mathcal{R}_d(x_r(t))$, respectively [20], i.e.,

$$\mathcal{J}_d = \begin{bmatrix} 0 & J_{12} & J_{13} \\ -J_{12} & 0 & J_{23} \\ -J_{13} & -J_{23} & 0 \end{bmatrix} \quad (4)$$

$$\mathcal{R}_d(x_r(t)) = \begin{bmatrix} r_1 & 0 & 0 \\ 0 & r_2 & 0 \\ 0 & 0 & r_3 \end{bmatrix} \quad (5)$$

leading to some solutions [19]. It follows that setting up $r_1 = x_2\alpha/x_1C^2$, $r_2 = 0$, $r_3 = R_l/L_l^2$, $J_{12} = -(\alpha/CC_{\mathrm{sc}})$, $J_{13} = -(1/CL)$, and $J_{23} = 0$ with $\alpha > 0$ leads to the nonlinear control law (see [19] for more design details) that matches regular controllers [25] based on PI controller, i.e.,

$$i_{\mathrm{fc}}^* = \frac{v_b}{\max\{v_{\mathrm{fc}}, v_{\mathrm{fc\ min}}\}} \left(\frac{v_b^*}{R_l} - \alpha\tilde{v}_{\mathrm{sc}} \right), \quad \alpha > 0 \quad (6)$$

$$i_{\mathrm{sc}}^* = -\alpha\tilde{v}_b. \quad (7)$$

Finally, the closed-loop system error is as follows:

$$\dot{\tilde{x}}_r(t) = [\mathcal{J}_d - \mathcal{R}_d(x_r(t))]\, \nabla H_d(\tilde{x}_r(t)) \quad (8)$$

with

$$\mathcal{J}_d = \begin{bmatrix} 0 & -\frac{\alpha}{CC_{\mathrm{sc}}} & -\frac{1}{LC} \\ \frac{\alpha}{CC_{\mathrm{sc}}} & 0 & 0 \\ \frac{1}{LC} & 0 & 0 \end{bmatrix}$$

$$\mathcal{R}_d(x_r(t)) = \begin{bmatrix} \frac{\alpha v_{\mathrm{sc}}}{C^2 v_b} & 0 & 0 \\ 0 & 0 & 0 \\ 0 & 0 & \frac{R_l}{L^2} \end{bmatrix}.$$

Remark 2: In [19], it has been shown that the outer closed-loop system is globally asymptotically stable. Moreover, according to Tikhonov's theorem [26], the whole system is locally asymptotically stable (see [19] for more details).

C. Practical Issues and Implementation

Equation (6) shows that FC current reference $u_{r1} = i_{\mathrm{fc}}^*$ is highly dependent on the load conductance. Consequently, the IDA-PBC would guarantee the dc bus voltage control by an estimation of the charge R_l. The proposed solution consists in the implementation of the following algorithm:

$$\hat{Y}_l = \frac{K_{Rl}}{s + K_{Rl}} \frac{i_l}{v_b} \quad (9)$$

$$i_{\mathrm{fc}}^*(t) = \frac{v_b(t)\left(v_b^*(t)\hat{Y}_l(t) - \alpha\tilde{v}_{\mathrm{sc}}(t) \right)}{\max\{v_{\mathrm{fc}}(t), v_{\mathrm{fc\ min}}\}} \quad (10)$$

$$i_{\mathrm{sc}}^*(t) = -\alpha\tilde{v}_b(t) \quad (11)$$

where an estimate of the conductance $Y_l = 1/R_l$ is implemented in order to avoid a division that is more computationally expensive than a multiplication. Gain K_{Rl} enables to adjust the sensitivity of control value $u_{r1}(t) = i_{\mathrm{fc}}^*(t)$ to R_l. Choosing a small parameter value ensures slow $i_{\mathrm{fc}}^*(t)$ variations even in the case of large $R_l(t)$ changes. In such a situation, strong variations of $i_{\mathrm{sc}}(t)$ ensure a good control of the bus voltage.

Remark 3: It could be noticed that the proposed controller needs an increase of sensors in order to measure the load current i_l compared with regular controller proposed in the literature. Nevertheless, in industrial applications, such current measurement could be useful to protect the equipment and ensure its reliability.

Remark 4: Stability analysis with a load estimator. The outer-loop voltage control composed of the third-order system (1), the load estimator, and the IDA-PBC is globally asymptotically stable, invoking a theorem on stability of cascaded systems (see [19] for more details).

Remark 5: The two sources have current and voltage limits. Consequently, saturation is included in the algorithm, as in [25].

Remark 6: The tuning of nonlinear controllers such as IDA-PBC is not obvious and trivial. To analyze the influence of the tuning parameters on the closed-loop system, more specifically on the FC current dynamics, some simulations have been carried out. After trials and errors, a reasonable choice for the two adjusting parameters α and K_r is (10,0.5). It ensures that the dynamic of the FC current is less than 4 A/s so that no significant impact on the ageing FC could be noticed [27]. It follows that the closed-loop bandwidths of the dc bus and SCs have been roughly evaluated nearly 1.6 and 0.25 Hz, respectively, ensuring the frequency decoupling of the two sources.

Specifically, the controller [see (9)–(11)] is implemented with a microcontroller, which involves sampled-data inputs $v_b[k]$ and $v_{\mathrm{fc}}[k]$, and control values $i_{\mathrm{fc}}^*[k]$ and $i_{\mathrm{sc}}^*[k]$ remained

constant between two consecutive sampling times by means of a ZOH device. The controller is

$$\hat{Y}_l[k] = e^{-K_{Rl}T_s}\hat{Y}_l[k-1] + (1-e^{-K_{Rl}T_s})\frac{i_l[k]}{v_b[k]} \quad (12)$$

$$i^*_{\rm fc}[k] = \frac{v_b[k]\left(v^*_b[k]\hat{Y}_l[k] - \alpha\tilde{v}_{\rm sc}[k]\right)}{\max\left\{v_{\rm fc}[k], v_{\rm fc\ min}\right\}} \quad (13)$$

$$i^*_{\rm sc}[k] = -\alpha\tilde{v}_b[k] \quad (14)$$

where T_s is the sampling period of the outer loop.

III. Sampled-Data IDA-PBC

A. Introduction

The passivity-based control technique developed in [28] has been further enhanced with the IDA-PBC methodology (see [29] and the references therein). Nevertheless, properties of the continuous controller are usually lost under sampling, leading to a decrement of the controller closed-loop performances. As a result, a direct sampled-data design, permitting the design of digital IDA-PBC in a quite systematic way, is more appropriate [22]. The sampled-data controller is designed in such a way that the energetic behavior of the sampled closed-loop system is equal to that of the continuous one at the sampling instant.

B. Sampled-Data Conception

The analysis of the interconnection and dissipation matrices shows that $\tilde{v}_b$ and $\tilde{v}_{\rm sc}$ are connected by the two inputs ($i^*_{\rm fc}$ and $i^*_{\rm sc}$) and ensure the stabilization of the continuous closed-loop system at the desired equilibrium point x^*_r with a good transient response. Therefore, the digital controller must preserve this energetic behavior by an appropriate design method.

Let us denote $\tilde{x}_r(t)$ and $u_r(t)$ the closed-loop continuous-time state and the control input, respectively, as detailed in Section II. The sampled state under control $u_r[k]$ is denoted, at the time instant $t = kT_s$, by $\tilde{x}_r[k]$. As stated in [22], the main idea is to design a sampled-data controller that reproduces the energetic behavior of the Hamiltonian function at the sample instants in order to guarantee the stability of the equivalent sampled-time closed-loop system.

Given a Hamiltonian function $H_d : \mathbb{R}^n \Longrightarrow \mathbb{R}$, $H_d(0) = 0$, and a continuous input $u_r(x_r(t))$ that ensures $\dot{H}_d(\tilde{x}_r(t)) \leq 0$, it is desired to design a constant piecewise control $u_r[k]$ to ensure, at the sampling instants

$$H_d\left(\tilde{x}_r[k+1]\right) - H_d\left(\tilde{x}_r[k]\right) = \int_{kT_s}^{(k+1)T_s} \dot{H}_d\left(\tilde{x}_r(\tau)\right) d\tau \quad (15)$$

with

$$\dot{H}_d\left(\tilde{x}_r(\tau)\right) = L_{f(\cdot)}H_d|_{\tilde{x}_r(\tau),t=\tau} \quad (16)$$

where L is the usual Lie derivative, and $f(\cdot) = (\mathcal{J}-\mathcal{R})Q\tilde{x}_r(t) + g(\tilde{x}_r(t) + x^*_r(t))u_r(t) + d(t)$.

The evolution of H_d in (16) reads

$$H_d\left(\tilde{x}_r\left((k+1)T_s\right)\right) = e^{T_s\pounds_{f(\cdot)}}H_d(\cdot)|_{\tilde{x}_r=\tilde{x}_r(kT_s),kT_s}. \quad (17)$$

Similarly, the evolution $\tilde{x}_r(\tau)$ of the continuous closed-loop system is defined as

$$\tilde{x}_r(\tau) = e^{(\tau-kT_s)\pounds_{f(\cdot)}}\tilde{x}_r|_{\tilde{x}_r=\tilde{x}_r(kT_s),kT_s} \quad (18)$$

where $\pounds_{f(\cdot)}$ is the Lie-Backlund derivative, which is defined according to the following recall.

Recall: [30] The first Lie-Backlund derivatives of any function $\Gamma(x,t)$ with respect to any vector field $\zeta(x,t)$ is defined as

$$\pounds_{\Gamma(x,t)}\zeta(x,t) = \frac{\partial\zeta(x,t)}{\partial x}\Gamma + \frac{\partial\zeta(x,t)}{\partial t}. \quad (19)$$

Iteratively, one has

$$\pounds^{j+1}_{\Gamma(x,t)}\zeta(x,t) = \pounds_{\Gamma(x,t)}\left(\pounds^{j}_{\Gamma(x,t))}\zeta(x,t)\right). \quad (20)$$

Now, considering the control $u_r(t) = u_r[k]$, the equilibrium point $x^*_r(t) = x^*_r[k]$, and the perturbation $d(t) = d[k]$ constants on the sampling interval, one obtains in (17)

$$H_d\left(\tilde{x}_r[k+1]\right) = e^{T_sL_{\tilde{f}(\cdot)}}H_d(\cdot)|_{\tilde{x}_r[k],k} \quad (21)$$

where $\pounds$ is replaced by the usual Lie derivative L (all the derivatives with respect to t are equal to zero), i.e., $\tilde{f}(\cdot) = (\mathcal{J}-\mathcal{R})Q\tilde{x}_r(t) + g(\tilde{x}_r(t) + x^*_r[k])u_r[k] + d[k]$.

In order to design the enhanced sampled controller, we look for a controller defined as follows:

$$u_r[k] = u_{r0}[k] + \sum_{i\geq 1}\frac{T_s}{(i+1)!}u_{ri}[k] \quad (22)$$

such that (16) holds when $x_r[k] = x_r(t)|_{t=kT_s}$.

It follows that, by equating homogeneous terms in powers of T_s in the right- and left-hand sides of (16), one iteratively computes each "corrective" term u_{ri} of the sampled-data controller, thus obtaining the following first terms:

$$u_{r0}[k] = u_c(t)|_{t=kT_s} \quad (23)$$

$$u_{r1}[k] = \dot{u}_c(t)|_{t=kT_s}. \quad (24)$$

The computation of higher order corrective term (i.e., $i \geq 2$) is unnecessary in practice. Therefore, an interesting solution can be proposed at the first order of approximation, i.e., $u_r[k]^T = [i^*_{\rm fc}[k]\ i^*_{\rm sc}[k]]^T$ with

$$\hat{Y}_l[k] = e^{-K_{Rl}T_s}\hat{Y}_l[k-1] + (1-e^{-K_{Rl}T_s})\frac{i_l[k]}{v_b[k]} \quad (25)$$

$$i^*_{\rm fc}[k] = \frac{v_b}{\max\{v_{\rm fc}, v_{\rm fc\ min}\}}\left(v^*_b\hat{Y}_l - \alpha\tilde{v}_{\rm sc}\right) + \frac{T_s}{2!}\gamma(\cdot)\Big|_{t=kT_s} \quad (26)$$

$$i^*_{\rm sc}[k] = -\alpha\tilde{v}_b + \frac{T_s}{2}\frac{\alpha}{C}\left(\alpha\frac{v_{\rm sc}}{v_b}\tilde{v}_b + \alpha\tilde{v}_{\rm sc} + \tilde{i}_l\right)\Big|_{t=kT_s} \quad (27)$$

with

$$\gamma(\cdot) = \dot{u}_c = -\alpha^2 \frac{v_b^* \tilde{v}_b}{C_{\rm sc} v_{\rm fc}} - \frac{1}{C_{\rm sc} v_{\rm fc}} \left(\alpha \frac{v_{\rm sc}}{v_b} \tilde{v}_b + \alpha \tilde{v}_{\rm sc} + \tilde{\tilde{i}}_l \right) \times \left(v_b^* \hat{Y}_l + \alpha \frac{v_{\rm sc}}{v_b} - 2\alpha \tilde{v}_{\rm sc} + \alpha v_{\rm sc}^* \right) \Big|_{t=kT_s} . \quad (28)$$

As a result, the proposed sampled-data controller $u_r[k]^T = [i_{\rm fc}^*[k], i_{\rm sc}^*[k]]^T$ computed as in (25)–(28) has better performances compared with the simple emulated controller because it improves to an error in $O(T_s^3)$ both the energetic performances ensuring convergency to the desired equilibrium (one step matching of the Hamiltonian function) and matching of the state variables evolutions at the sampling instants. These performances are discussed and well illustrated in Section IV through real implementation tests.

However, due to the interplay between the sampling period length and how far one is from the equilibrium, one cannot theoretically prove asymptotic convergency under approximate digital controller. It is reasonable to conjecture that, as usual, in such a context, some practical stability such as condition holds at the sampling instants.

C. Practical Implementation

In practice, the controller leads to a flat variation of the FC current. Hence, the corrective input $\gamma(v_b, v_{\rm sc}, i_l, Y_l) = \dot{u}_c$ is rather low, thus possible to neglect without compromising on the performances. Conversely, the $i_{\rm sc}^*$ corrective term may produce high values. This latter becomes important in case of large sampling period.

Finally, the practical proposed sampled-data controller $u_r[k]^T = [i_{\rm fc}^*[k], i_{\rm sc}^*[k]]^T$ is defined as follows:

$$\hat{Y}_l[k] = e^{-K_{Rl} T_s} \hat{Y}_l[k-1] + (1 - e^{-K_{Rl} T_s}) \frac{i_l[k]}{v_b[k]} \quad (29)$$

$$i_{\rm fc}^*[k] = \frac{v_b}{\max\{v_{\rm fc}, v_{\rm fc\,min}\}} \left(v_b^* \hat{Y}_l - \alpha \tilde{v}_{\rm sc} \right) \Big|_{t=kT_s} \quad (30)$$

$$i_{\rm sc}^*[k] = -\alpha \tilde{v}_b + \frac{T_s}{2} \frac{\alpha}{C} \left(\alpha \frac{v_{\rm sc}}{v_b} \tilde{v}_b + \alpha \tilde{v}_{\rm sc} + \tilde{\tilde{i}}_l \right) \Big|_{t=kT_s} . \quad (31)$$

IV. Experimental Results

A. Test Bench Description

The experimental setup (see Table I) is based on a Nexa Ballard FC (46 A/1200 W) associated with two Maxwell SC modules in series (125 F). The FC and SC boost converters are based on metal–oxide–semiconductor field-effect transistor modules switching at 20 kHz. The load is emulated by a programmable electronic equipment from Höcherl & Hackl (model ZS1806, rated power of 1800 W, imax = 150 A, Vmax = 60 V). Finally, the controllers are implemented in a dSPACE DS1103 board where the voltage outer control loops sampling has been set to 20 kHz or 500 Hz. The current closed loops are based on PI controller updated at 20 kHz [17], [19].

TABLE I
Electric Characteristics of the Hybrid System

Fuel cell parameters			
Open circuit voltage E	45 V	v_{fcmin}	26 V
Rated voltage	26 V	Rated current	46 A
Supercapacitors parameters			
Capacitance	125 F	v_{sc}^*	21 V
Rated voltage	30 V	Rated current	200 A
Electric load parameters			
Rated voltage	60 V	Rated current	150 A
Rated power	1800 W		
Inductance and capacity parameters			
L_{fc} inductance	200 μH	L_{sc} inductance	100 μH
Rated current L_{fc}	100 A	Rated current L_{sc}	150 A
Capacity C	9 mF	Inductance L	1 mH
v_b^*	50 V		
Control parameters			
Kp_{fc}	0.030	Ki_{fc}	30
Kp_{sc}	0.030	Ki_{sc}	30
α	10	K_{Rl}	0.5

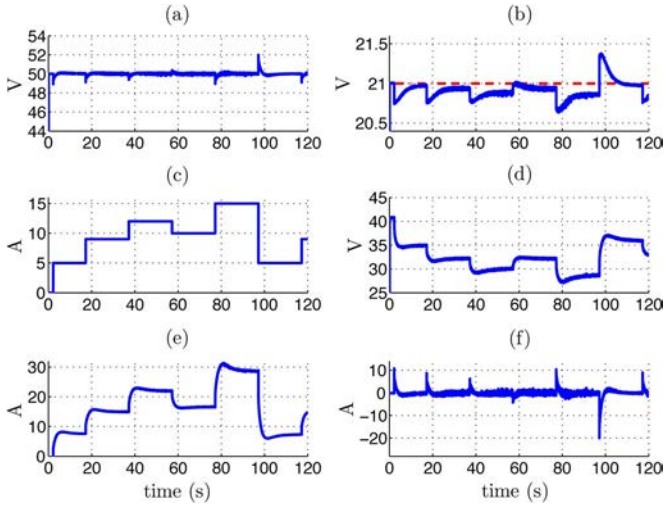

Fig. 2. Experimental result of the emulated controller—$T_s = 50$ μs. (a) bus voltage v_b. (b) SCs voltage $v_{\rm sc}$. (c) load current i_l. (d) fuel cell voltage $v_{\rm fc}$. (e) fuel cell current $i_{\rm fc}$. (f) SCs current $i_{\rm sc}$.

B. Result Analysis

All the experimental results detailed thereafter have been performed in order to validate the outer-loop control algorithm. Hence, in order to highlight the performances of the new digital controller, a comparison between the emulated controller based on the continuous-time design [implementation of the continuous IDA-PBC with a ZOH device, (12)–(14)] and the sampled-data controller (29)–(31) are detailed for different sampling periods.

Figs. 2 and 3 show the responses of the emulated controller for sampling periods equal to 50 μs and 2 ms, respectively, where the dc bus voltage reference is set equal to 50 V, and the load current varies between 0 and 15 A (this is equivalent to a load admittance variation from 0 to 0.3 S).

First, all the abrupt variations of the power load at time 1, 16, 36, 76, or 116 s have been balanced by an abrupt variation of the SC current [see Figs. 2(f) and 3(f)], ensuring that the dc bus reference voltage is reached [see Figs. 2(a) and 3(a)]. On the contrary, any load power decrease (at $t = 56$ or 96 s) leads to

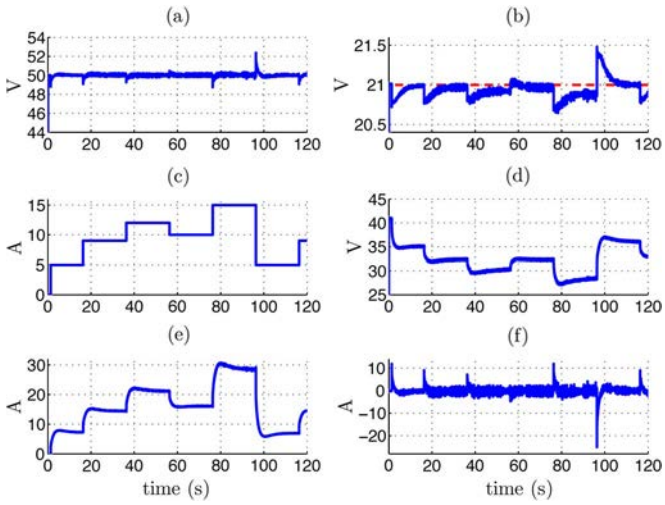

Fig. 3. Experimental result of the emulated controller—$T_s = 2$ ms. (a) bus voltage v_b. (b) SCs voltage $v_{\rm sc}$. (c) load current i_l. (d) fuel cell voltage $v_{\rm fc}$. (e) fuel cell current $i_{\rm fc}$. (f) SCs current $i_{\rm sc}$.

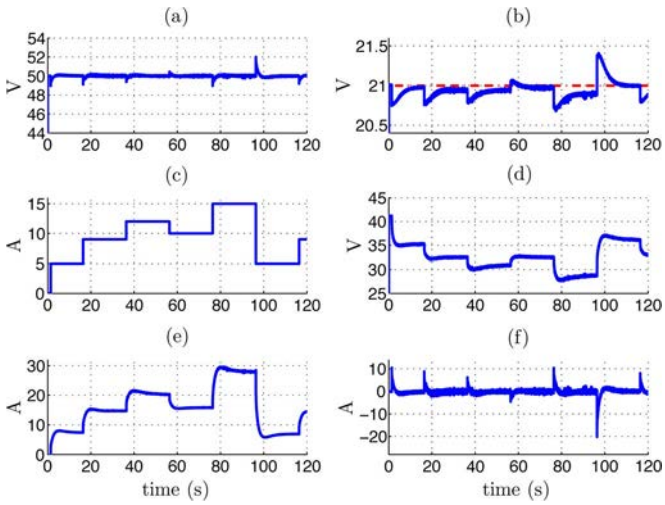

Fig. 4. Experimental result of the sampled-data controller—$T_s = 50$ μs. (a) bus voltage v_b. (b) SCs voltage $v_{\rm sc}$. (c) load current i_l. (d) fuel cell voltage $v_{\rm fc}$. (e) fuel cell current $i_{\rm fc}$. (f) SCs current $i_{\rm sc}$.

a slow decrease in FC current $i_{\rm fc}$ and, thereafter, a recharge of the SCs with the excess of energy.

Second, we can note that the SC voltage is not perfectly equal to its reference at steady state. In fact, the controller design supposes that the converters are lossless (no perturbation) and all the parameters are well known. Therefore, in practice, this small steady-state error could be removed by adding a small integral term without deteriorating the stability [19], [31].

Third, the remaining useful life of the FC is ensured by the smooth variation of the current $i^*_{\rm fc}$ (adjusted by gain K_{Rl}) despite rapid power load requests.

Fourth, it can be noticed that the increase in the sampling period amplifies the peak of the SCs' current and the signals' noise.

Figs. 4 and 5 show the responses of the sampled-data controller for sampling periods equal to 50 μs and 2 ms, respectively. We can notice that the sampled-data controller prevents overshoots of the SC current and the dc bus voltage,

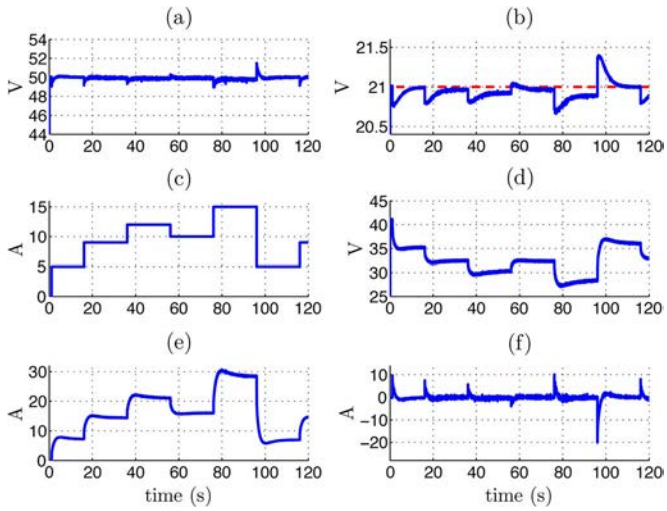

Fig. 5. Experimental result of the sampled-data controller—$T_s = 2$ ms. (a) bus voltage v_b. (b) SCs voltage $v_{\rm sc}$. (c) load current i_l. (d) fuel cell voltage $v_{\rm fc}$. (e) fuel cell current $i_{\rm fc}$. (f) SCs current $i_{\rm sc}$.

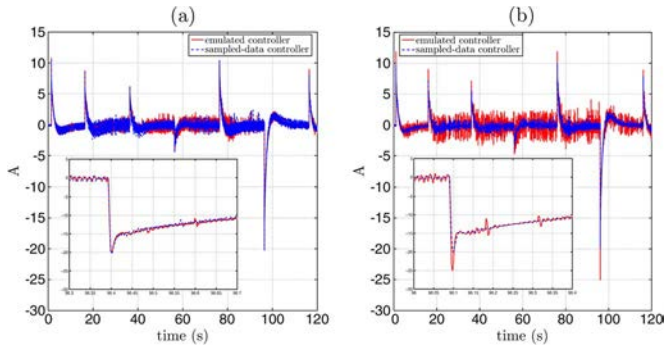

Fig. 6. Experimental result of the emulated and sampled-data controllers. (a) SCs current $i_{\rm sc}$ – $T_s = 500$ μs. (b) SCs current $i_{\rm sc}$ – $T_s = 2$ ms.

although the sampling frequency is significantly reduced. In conclusion, the performances are maintained with the sampled-data controller,, whereas the emulated algorithm greatly reduces them.

Indeed, for a sampling time equal to 2 ms, the emulated controller has an SC peak current $i_{\rm sc}^{\rm max}$ at about 11.85 A at $t = 1$ s, as opposed to the sampled-data controller, which only induces a 9.67-A peak. An analog observation can be noticed at $t = 96$ s during a load power decrease. The emulated controller requests a $i_{\rm sc}^{\rm min} = -25$ A, whereas sampled-data controller requests $i_{\rm sc}^{\rm min} = -20$ A. These observations are illustrated in Fig. 6. This confirms that the proposed controller is actually effective in a sampled-data context. Using the sampled-data controller leads to very satisfactory performances of the equipment under control, and this is increasingly so when the sampling period is high.

V. Conclusion

Motivated by recent theoretical results from sampled passivity-based control, a new controller for coordination of an FC and SCs has been detailed. Practical results show that the performances of the system under control with an emulated controller have been downgraded when the sampling frequency

has been reduced. By contrast, in the same context, the sampled IDA-PBC has maintained the requested performance. It follows that such controller is suitable for high-power industrial applications where the switching and sampling frequencies are low.

REFERENCES

[1] S. Caux, J. Lachaize, M. Fadel, P. Shott, and L. Nicod, "Modelling and control of a fuel cell system and storage elements in transport applications," *J. Process Control*, vol. 15, no. 4, pp. 481–491, Jun. 2005.

[2] P. Rodatz, G. Paganelli, A. Sciarretta, and L. Guzzella, "Optimal power management of an experimental fuel cell/supercapacitor-powered hybrid vehicle," *Control Eng. Practice*, vol. 13, no. 1, pp. 41–53, Jan. 2005.

[3] P. Thounthong, S. Rael, and B. Davat, "Control strategy of fuel cell and supercapacitors association for a distributed generation system," *IEEE Trans. Ind. Electron.*, vol. 54, no. 6, pp. 3225–3233, Nov. 2007.

[4] R. Malo and R. Griñó, "Design, construction, control of a stand-alone energy-conditioning system for PEM-type fuel cells," *IEEE Trans. Power Electron.*, vol. 25, no. 10, pp. 2496–2506, May 2010.

[5] A. Shahin *et al.*, "High voltage ratio dc–dc converter for fuel-cell applications," *IEEE Trans. Ind. Electron.*, vol. 57, no. 12, pp. 3944–3955, Mar. 2010.

[6] X. Zhu, X. Li, G. Shen, and D. Xu, "Design of the dynamic power compensation for PEM FC distributed power system," *IEEE Trans. Ind. Electron.*, vol. 57, no. 6, pp. 1935–1944, Feb. 2010.

[7] M. Ghanes, M. Hilairet, J.-P. Barbot, and O. Béthoux, "Singular perturbation control for coordination of converters in a fuel cell system," in *Proc. Electrimacs*, 2011, pp. 1–6.

[8] M. Hilairet and O. Béthoux, "A passive controller-observer for coordination of converters in a fuel cell system," in *Proc. IEEE ISIE*, Bari, Italy, Jul. 2011, pp. 2209–2214.

[9] S. Mariéthoz, O. Béthoux, and M. Hilairet, "A distributed model predictive control scheme for reducing consumption of hybrid fuel cell systems," in *Proc. IEEE IECON*, Oct. 2012, pp. 868–873.

[10] P. Garca, J. Torreglosa, L. Fernandez, and F. Jurado, "Control strategies for high-power electric vehicles powered by hydrogen fuel cell, battery and supercapacitor," *Expert Syst. With Appl.*, vol. 40, no. 12, pp. 4791–4804, Sep. 2013.

[11] M. Jang, M. Ciobotaru, and V. Agelidis, "Design and implementation of digital control in a fuel cell system," *IEEE Trans. Ind. Electron.*, vol. 9, no. 2, pp. 1158–1166, Oct. 2013.

[12] S. Koohi-Kamali, V. Tyagi, N. Rahim, N. Panwar, and H. Mokhlis, "Emergence of energy storage technologies as the solution for reliable operation of smart power systems: A review," *Renew. Sustainable Energy Rev.*, vol. 25, pp. 135–165, Sep. 2013.

[13] A. Tani, M. B. Camara, B. Dakyo, and Y. Azzouz, "DC/DC and dc/ac converters control for hybrid electric vehicles energy management—Ultracapacitors and fuel cell," *IEEE Trans. Ind. Informat.*, vol. 9, no. 2, pp. 686–696, May 2013.

[14] J. Torreglosa, P. Garcia, L. Fernandez, and F. Jurado, "Predictive control for the energy management of a fuel cell-battery-supercapacitor tramway," *IEEE Trans. Ind. Informat.*, vol. 10, no. 1, pp. 276–285, Feb. 2014.

[15] M. Ghanes, O. Bethoux, M. Hilairet, and J. Barbot, "Fuel cell system control under converter losses with experimental results," in *Proc. 19th IFAC World Congr.*, Aug. 24–29, 2014, pp. 1–9.

[16] S. N. Motapon, L.-A. Dessaint, and K. Al-Haddad, "A comparative study of energy management schemes for a fuel-cell hybrid emergency power system of more-electric aircraft," *IEEE Trans. Ind. Electron.*, vol. 61, no. 3, pp. 1320–1334, Apr. 2014.

[17] T. Azib, O. Béthoux, G. Remy, C. Marchand, and E. Berthelot, "An innovative control strategy of a single converter for hybrid fuel cell/supercapacitors power source," *IEEE Trans. Ind. Electron.*, vol. 57, no. 12, pp. 4024–4031, Dec. 2010.

[18] P. Thounthong, S. Rael, B. Davat, and P. Sethakul, "Fuel cell high-power applications," *IEEE Ind. Electron. Mag.* , vol. 3, no. 1, pp. 32–46, Mar. 2009.

[19] M. Hilairet *et al.*, "A passivity-based controller for coordination of converters in a fuel cell system," *Control Eng. Practice*, vol. 21, no. 8, pp. 1097–1109, Aug. 2013.

[20] R. Ortega and E. Garcia-Canseco, "Interconnection and damping assignment passivity-based control: A survey," *Eur. J. Control*, vol. 10, no. 5, pp. 432–450, 2004.

[21] S. Monaco, D. Normand-Cyrot, and F. Tiefensee, "Sampled-data stabilization; a PBC approach," *IEEE Trans. Autom. Control*, vol. 56, no. 4, pp. 907–912, Dec. 2010.

[22] F. Tiefensee, S. Monaco, and D. Normand-Cyrot, "IDA-PBC under sampling for port-controlled Hamiltonian systems," in *Proc. ACC*, 2010, pp. 1811–1816.

[23] F. Tiefensee, M. Hilairet, D. Normand-Cyrot, and O. Béthoux, "Sampled-data energetic management of a fuel cell/supercapacitor system," in *Proc. IEEE VPPC*, 2010, pp. 1–6.

[24] P. Kokotovic, H. Khalil, and J. O'Reilly, *Singular Perturbation Methods in Control: Analysis and Design*. New-York, NY, USA: Academic, 1986.

[25] T. Azib, O. Béthoux, G. Remy, and C. Marchand, "Structure and control strategy for a parallel hybrid fuel cell/supercapacitors power source," in *Proc. IEEE VPPC*, Sep. 2009, pp. 1858–1863.

[26] A. Tikhonov, A. Vasil'eva, and V. Volosov, *Ordinary Differential Equations*, *Mathematics Applied to Physics*, E. Roubine, Ed. New York, NY, USA: Springer-Verlag, 1970.

[27] B. Wahdame *et al.*, "Comparison between two PEM fuel cell durability tests performed at constant current under solicitations linked to transport mission profile," *Int. J. Hydrogen Energy*, vol. 32, no. 17, pp. 4523–4536, Dec. 2007.

[28] R. Ortega and M. Spong, "Adaptive motion control of rigid robots: A tutorial," *Automatica*, vol. 25, no. 6, pp. 877–888, Nov. 1989.

[29] R. Ortega, A. V. der Schaft, B. Maschke, and G. Escobar, "Interconnection and damping assignment passivity based control of port controlled Hamiltonian systems," *Automatica*, vol. 38, no. 4, pp. 585–596, Apr. 2002.

[30] M. Fliess, J. Lévine, and P. Rouchon, "A Lie-Bäcklund approach to equivalence and flatness of nonlinear systems," *IEEE Trans. Autom. Control*, vol. 44, no. 5, pp. 922–937, May 1999.

[31] A. Donaire and S. Junco, "On the addition of integral action to port-controlled Hamiltonian systems," *Automatica*, vol. 45, no. 8, pp. 1910–1916, Aug. 2009.